Simulating Water Retention Characteristics with Lattice Boltzmann Methods

Marcel Schaap[1], Mark L. Porter[2], Britt S.B. Christensen[3], and Dorthe Wildenschild[2].

[(1)] Dept. of Soil, Water and Environmental Science, University of Arizona, University of Arizona, Tucson, AZ 85721.

[(2)] Dept. of Civil, Construction, and Environmental Engineering, Oregon State University, Corvallis, OR 97331

[(3)] Dept. of Hydrology, Geological Survey of Denmark and Greenland (GEUS), Øster Voldgade 10, DK-1350 Copenhagen, Denmark

ABSTRACT

In this presentation we compare observed and simulated water retention characteristics. Observed data were obtained for water-air displacement in a glass-bead system with the Advanced Photon Source synchrotron at DOE's Argonne laboratory at a resolution of 17 microns. Simulated water retention characteristics were generated with a Lattice Boltzmann model that is able to calculate flow and interfacial phenomena at the pore scale. We show that there is good match between observations and simulations for both drainage and wetting data.

OBJECTIVE

Recent progress in observational and computational techniques has advanced studies of of fluid dynamics and interfacial geometry in porous media. Computational advances largely concern Lattice Boltzmann (LB) method which can simulating microscale flow in porous media by approximating the Navier-Stokes equation. With some extensions, the LB method is also able to deal with microscale interfacial phenomena in single or multiphase or multi component systems.

The objective of this paper is to demonstrate that water retention curves can be computed directly from pore-space geometry and fundamental fluid properties.

We do this by applying LB modeling to an observed microscale multiphase pore geometry obtained by *Culligan et al.* [2004, 2006] and to compare observed and simulated pressure-saturation characteristics with a Shan-Chen-type two-component model.

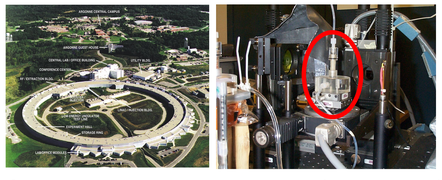

Figure 1. *Argonne APS synchrotron and experimental setup with glass bead column.*

P_c=980 Pa drainage for every 5'th image

EXPERIMENTAL DATA

The water-air displacement experiments were carried out at the GeoSoilEnviro Consortium for Advanced Radiation Sources (GSECARS) bending magnet beamline, Advanced Photon Source, Argonne National Laboratory. An acrylic column (70 mm tall, 7 mm inner diameter) was filled with soda-lime glass beads with sizes between 0.6 to 1.4 mm (Figure 1). A pressure transducer at the outflow channel measured the capillary pressure, while a syringe pump was used to pump a precise amount of water into or out of the sample at predetermined rates. The top of the sample was connected to the open air.

Computed microtomography (CMT) using 33 keV monochromatic X-ray radiation was used to image the three-dimensional distribution of solid, wetting, and non-wetting phases at a resolution of 17 μm^3 per voxel. Water was doped with a 0.1 M KI solution to enhance contrast between the fluid and solid phase. Because of experimental and computational constraints it was only possible to image the middle 5 mm of the column. The LB modeling focuses only on the top 1.7 mm of this section (100 slices). This volume should contain at least two REVs according to data by *Culligan et al.* [2004].

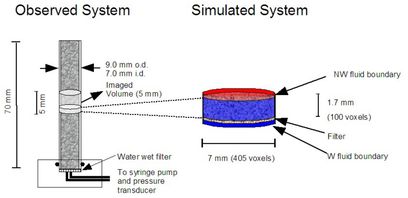

Figure 2. *Schematic overview of experimental setup and model implementation.*

LATTICE BOLTZMANN MODEL

The D3Q19 model [*Qian et al.*, 1992; *Martys and Chen*, 1996] implements a 3D model consisting of a regular lattice of nodes. Each node maintains a particle distribution, $f_i(\mathbf{x},t)$, where the subscript i is the index of the 19 members, 18 of which form links that point to neighboring nodes with relative positions indicated by the vectors $\mathbf{e}_i$ (Fig. 3); $\mathbf{x}$ is the discrete location of each node (x, y, z coordinates), and t is time. Distribution member 0 is essentially a rest mass.

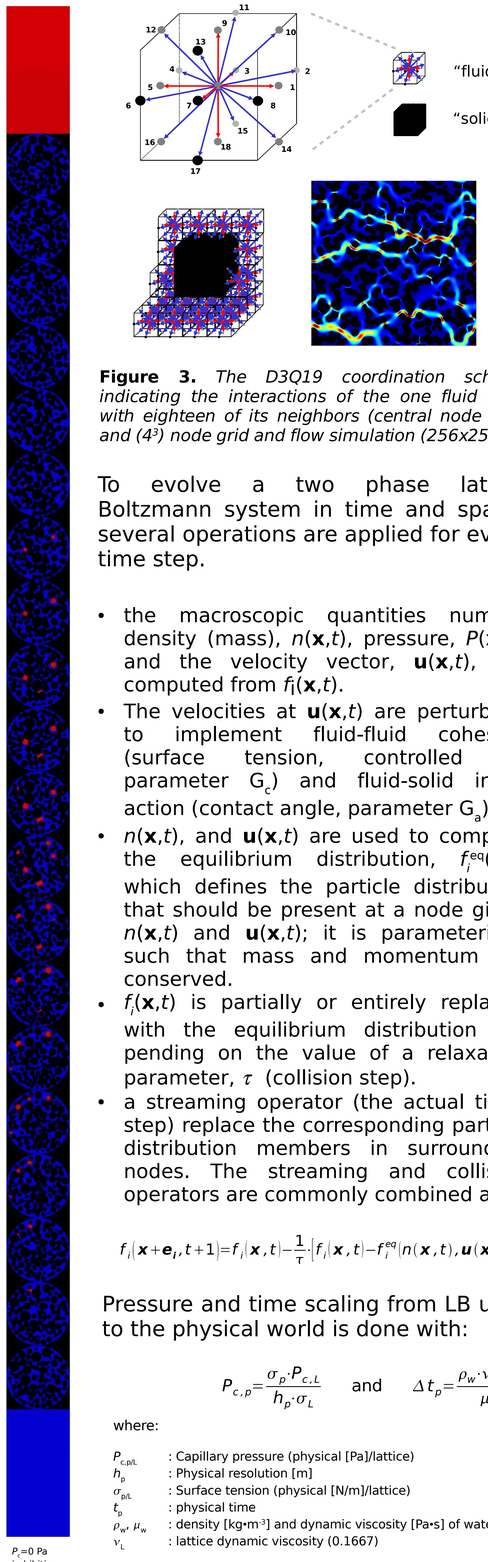

P_c=0 Pa imbibition for every 5'th image

Figure 3. *The D3Q19 coordination scheme indicating the interactions of the one fluid node with eighteen of its neighbors (central node is 0) and (4^3) node grid and flow simulation (256x256).*

To evolve a two phase lattice Boltzmann system in time and space, several operations are applied for every time step.

- the macroscopic quantities number density (mass), $n(\mathbf{x},t)$, pressure, $P(\mathbf{x},t)$, and the velocity vector, $\mathbf{u}(\mathbf{x},t)$, are computed from $f_i(\mathbf{x},t)$.
- The velocities at $\mathbf{u}(\mathbf{x},t)$ are perturbed to implement fluid-fluid cohesion (surface tension, controlled by parameter G_c) and fluid-solid interaction (contact angle, parameter G_a).
- $n(\mathbf{x},t)$, and $\mathbf{u}(\mathbf{x},t)$ are used to compute the equilibrium distribution, $f_i^{eq}(\mathbf{x},t)$ which defines the particle distribution that should be present at a node given $n(\mathbf{x},t)$ and $\mathbf{u}(\mathbf{x},t)$; it is parameterized such that mass and momentum are conserved.
- $f_i(\mathbf{x},t)$ is partially or entirely replaced with the equilibrium distribution depending on the value of a relaxation parameter, τ (collision step).
- a streaming operator (the actual time-step) replace the corresponding particle distribution members in surrounding nodes. The streaming and collision operators are commonly combined as:

$$f_i(\boldsymbol{x}+\boldsymbol{e}_i, t+1) = f_i(\boldsymbol{x},t) - \frac{1}{\tau}\cdot\left[f_i(\boldsymbol{x},t) - f_i^{eq}(n(\boldsymbol{x},t), \boldsymbol{u}(\boldsymbol{x},t))\right]$$

Pressure and time scaling from LB units to the physical world is done with:

$$P_{c,p} = \frac{\sigma_p \cdot P_{c,L}}{h_p \cdot \sigma_L} \quad \text{and} \quad \Delta t_p = \frac{\rho_w \cdot \nu_L \cdot h_p^2}{\mu_w}$$

where:

$P_{c,p/L}$	: Capillary pressure (physical [Pa]/lattice)
h_p	: Physical resolution [m]
$\sigma_{p/L}$	: Surface tension (physical [N/m]/lattice)
t_p	: physical time
ρ_w, μ_w	: density [kg•m^{-3}] and dynamic viscosity [Pa•s] of water
ν_L	: lattice dynamic viscosity (0.1667)

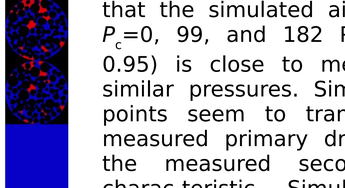

P_c=540 Pa drainage for every 5'th image

RESULTS

To set the contact angle parameter G_a we enclosed equal masses of wetting fluid (blue) and a non-wetting fluid (red) in a closed capillary consisting of a 3D square duct. The top row in Figure 4 shows that the contact angle changed from 90 degrees at G_a=0 (neither fluid is wetting or non-wetting) to zero at G_a =0.012. The red non-wetting fluid detaches from the wall and an increasingly thicker film is formed for G_a >0.012.

Time series of wetting phase saturations for drainage or imbibition steps show that hundreds of thousands of iterations were needed to reach (near-) equilibrium (fig 5). This corresponds to about 25 to 50 seconds of physical time. Each simulation took approximately four weeks on a four-CPU AMD64 system, total CPU time for this poster was approximately two years.

Profiles of average wetting phase saturation for the P_c=980 Pa drainage step is shown in Figure 5A. Likewise, Figure 5B shows data for the P_c=0 Pa imbibition step. Final saturation profiles of all simulations appear in Fig 5C and 5D. For drainage the NW phase does not percolate to the bottom of the sample for pressures of 91, 182, 272, 362, and 453 Pa, making it difficult to assign a representative saturation for these simulations. Figure 5D shows that, the saturation profiles for imbibition are more uniform with depth. NW phase entrapment is clearly visible for 0, 99, and 182 Pa.

Measured pressure-saturation data from *Culligan et al.* [2004] along with simulated results for the water-air and water-Soltrol systems appear in Fig. 6A. The water-air graph shows an encouraging correspondence between the observations and the simulations. Imbibition points match the observed data well and it is interesting to note that the simulated air entrapment at P_c=0, 99, and 182 Pa (saturation is 0.95) is close to measured data at similar pressures. Simulated drainage points seem to transition from the measured primary drainage curve to the measured secondary drainage charac-teristic. Simulated secondary drainage points are in good agreement with the measured data.

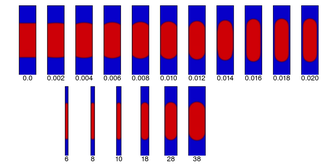

Figure 4. *Control over contact angles.*

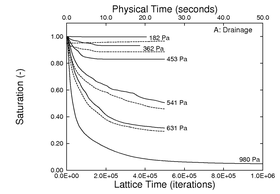

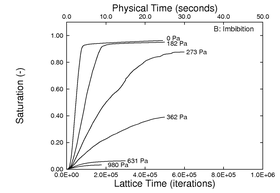

Figure 4. *Drainage (top) and imbibition saturation time series..*

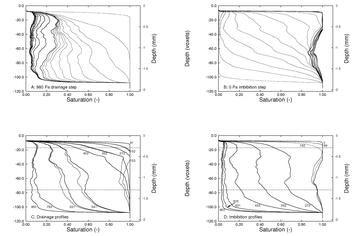

Figure 5. *Drainage and imbibition saturation profile time series (top) and final saturation profiles (bottom).*

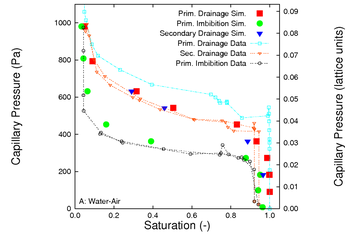

Figure 6. *Observed (CMT) and computed (LB) pressure saturation characteristics for drainage and imbibition.*

Acknowledgments

We thank the GeoSoilEnviro Consortium for Advanced Radiation sources (GSECARS) bending magnet beamline, Sector 13, Advanced Photon Source, Argonne National Laboratory. Wildenschild and Porter were supported, in part, by NSF-EAR-0337711 and NSF-EAR-0610108. Schaap was supported, in part, by NSF-EAR-0337378, NSF-EAR-061003, NWO-ALW in the Netherlands and USDA-ARS Salinity Laboratory, Riverside, California.